Synthesis and optical properties of Mn-doped CaWO$_4$ nanoparticles

P Suneeta[1], R Ajay Kumar[1], M V Ramana[2], G Kiran Kumar[3], Anindita Chatterjee[4] and Ch Rajesh[5]

[1] Advanced Functional Materials Laboratory, Department of Physics, Koneru Lakshmaiah Education Foundation, Vaddeswaram, Andhra Pradesh, 522 502, India
[2] Department of Physics, S R Govt. Arts & Science College, Kothagudem, Telangana, India
[3] Department of Physics, Raghu Engineering College (A), Visakhapatnam, 531162, India
[4] Department of Chemistry, Raghu Engineering College (A), Visakhapatnam, 531162, India
[5] Department of Physics, Gayatri Vidya Parishad College of Engineering (Autonomous), Madhurwada, Visakhapatnam, 530 048, India

E-mail: rajesh8112@gmail.com

Abstract

Pure and Mn-doped calcium tungstate (Mn:CaWO$_4$) nanoparticles (NPs) were synthesized by hydrothermal method which lead to the formation of high quality and narrow sized particles. The concentration of Mn in CaWO$_4$ NPs was varied from 1% to 4% by weight. A distinct peak of Mn (d–d) transition was observed which is actually spin-forbidden but may be allowed due to crystal field effects. Electron spin resonance measurements revealed inclusion of Mn^{2+} at the substitutional site.. Room temperature photoluminescence emission (PL) and excitation (PLE) spectroscopies were carried out to understand the interactions of sp-d levels. PL spectra revealed the presence of both band-edge ($\sim$450 nm) and Mn^{2+} related orange luminescence ($\sim$530 nm). Time dependent photoluminescence (TDPL) studies were also carried out where the life time value of 4.3 ms obtained was in accordance with measurement for Mn in other systems. Thus TDPL further strengths the presence of Mn in 2+ state in CaWO$_4$ NPs.

Supplementary material for this article is available online

(Some figures may appear in colour only in the online journal)

1. Introduction

It has been over a decade that the metal tungstates nanoparticles (NPs) have attracted a lot of interest because of their exciting properties [1] such as good chemical stability, relatively high refractive index, large absorption coefficient and high quantum yield. Tungstate crystals have been divided into two groups depending upon the size of the metal cation as well as their structure. If the metal cation has an ionic radius less than 0.77°A (Mg, Zn) they form monoclinic wolframite structure and that metal ion which have larger ionic radius than 0.77 °A (Ca, Ba) forms tetragonal scheelite structure [2]. Of all the metal tungstates, calcium tungstate (CaWO$_4$) is treated as the most potential material. CaWO$_4$ with scheelite structure emits in blue region and can be used as blue phosphor which is an important optical material. Due to this emission in the blue region it has wide range of applications as scintillating materials for detecting x-rays, γ-rays for medical applications and in oscilloscopes, in industrial radiology, medical diagnosis and as a sensor for dark matter research [3–8].

The luminescence property of CaWO$_4$ NPs were analyzed and reported by Anukorn *et al* [9]. The photoluminescence (PL) emission peak was found to be around 422 nm (which is in blue region) and the emission was attributed to the $^1T_2 \rightarrow {}^1A_1$ transition in the [WO4]$^{2-}$ excited complexes [9]. Later on by using different methods such as solid-state method [10], co-precipitation [11], solvo-thermal

1

[12], sol-gel [13], reverse micellar reactions [14], microwave hydrothermal [11], combustion and hydrothermal [15] synthesis of CaWO$_4$ NPs were carried out. Till now most of the work has been concentrated around doping a rare earth element into CaWO$_4$ NPs [15–17]. The reason for doping rare earth element may be attributed to their high energy transfer between them and the host lattice, because of which these materials are the best candidates for luminescent applications. To the best of our knowledge most of the work carried out on CaWO$_4$ NPs is on doping rare earth element into the host lattice [18, 19]. Reported work on doping of transition metal has been limited to preparation of bulk material [20, 21]. Electron paramagnetic resonance spectra and time dependent photoluminescence studies to prove Mn inclusion in CaWO4 NP lattice in its 2+ state has never been reported. In this work we made an attempt to dope a transition metal in order to exploit the usage of these NPs for white light generation as in our earlier work where both copper (Cu) and Mn were doped in ZnSe quantum dots to achieve white light generation [22]. In this regard an attempt was made initially to dope Mn in CaWO$_4$ NPs and to see its feasibility. In our future work dual dopants (Cu and Mn) will also be tried for white light generation.

Thus Mn doped CaWO$_4$ NPs were synthesized by hydrothermal method. These NPs were then analyzed for structural as well as optical properties. Electron spin resonance (ESR) and time dependent photoluminescence studies were also carried out on these NPs to ensure that manganese has been incorporated in to the lattice of CaWO$_4$.

2. Materials and methods

Synthesis of Mn-doped CaWO$_4$ (Mn:CaWO$_4$) NPs was carried out by adopting hydrothermal method with slight modification [15]. The precursors used here were purchased from Sigma Aldrich and were of analytical grade. No further purification was done. Initially in a beaker a sodium oleate (C$_{18}$H$_{33}$NaO$_2$) along with ammonium metatungstate hydrate (NH$_4$)$_6$H$_2$W$_{12}$O$_{40}$ were stirred by adding desired amount of double distilled water in order to prepare a solution. In the next step, another solution was made by mixing oleic acid and isopropyl alcohol and allowed it to stir for an hour. After one hour of stirring both the solutions were mixed together (solution 1). To obtain pure CaWO$_4$ NPs anhydrous calcium nitrate (Ca(NO$_3$)$_2$) was added to the above solution. Whereas for the case of doping calculated amount of anhydrous manganese nitrate (Mn(NO$_3$)$_2$) was also added along with Ca(NO$_3$)$_2$ and mixed with double distilled water to prepare another solution 2. The solution 2 thus prepared was then introduced into solution 1 and allowed it to stir for 30 min. Further the entire solution was transferred into an autoclave which was sealed and heated to 180 °C for 12 h. As soon as the temperature of the auto clave dropped down to room temperature the product was centrifuged. The powder obtained after centrifugation was allowed to dry in furnace at 100 °C for 3 h which resulted in light pink color of the
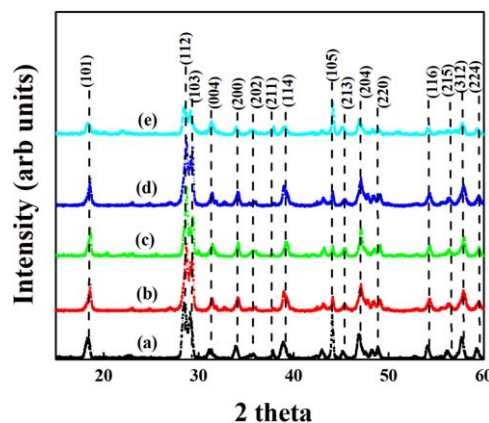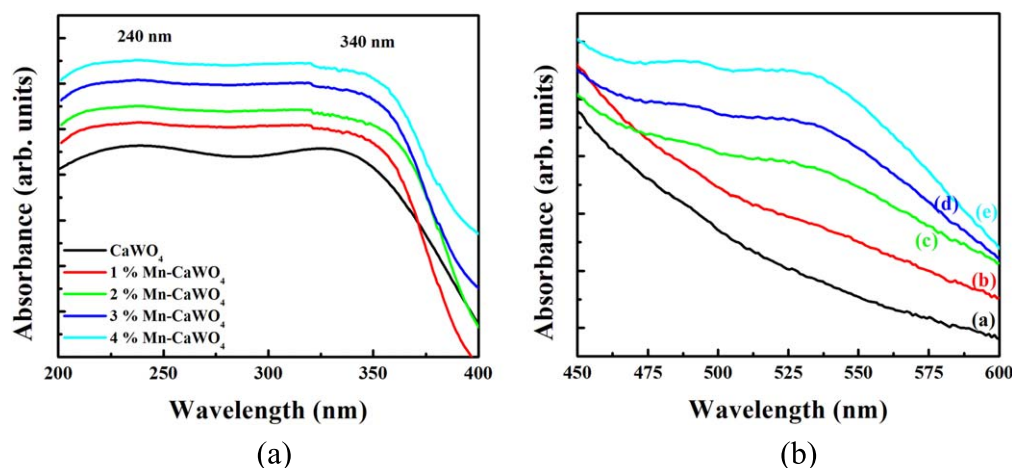

Figure 1. XRD pattern of (a) CaWO$_4$, (b) 1% Mn: CaWO$_4$, (c) 2% Mn: CaWO$_4$, (d) 3% Mn: CaWO$_4$ and (e) 4% Mn: CaWO$_4$ NPs respectively.

sample. The as obtained powder was further used for all characterizations.

Pure and Mn-doped CaWO$_4$ NPs phase analysis is done using x-ray diffraction (XRD) technique and for that a Philips PW 1840 powder x-ray diffractometer with Cu K$_\alpha$ line used as an incident radiation. A Bruker EMX spectrometer operating at 9.1 GHz was used for ESR measurement which was operated at liquid nitrogen temperature. Band gap related studies were carried out for both pure and Mn-doped CaWO$_4$ NPs with the help of JASCO V-670 in the range of 200–800 nm. To get the information related to band-edge and defect related emission photoluminescence emission, excitation spectra were carried out on spectrophotometer of JASCO FP8300. Time-resolved photoluminescence measurements were carried out on Edinburg instruments, FLSP920 system operating at 6.8 kV and with a pulse frequency of 40 kHz. The NPs were excited with nanosecond as well as millisecond flash lamp. All the characterizations were done by taking Mn doped CaWO$_4$ NPs in powder form only.

3. Results and discussion

Figure 1 reveals the XRD patterns of pure as well as Mn-doped CaWO$_4$ NPs with different molar concentrations of Mn (1%–4% by weight). These patterns revealed that the NPs possessed high crystallinity, were formed in tetragonal phase and matched well with the JCPDS (JCPDS No. 41–1431) data of bulk CaWO$_4$ which were in $I4_1/a$ space group. Even upon incorporation of Mn in to the host lattice (CaWO$_4$) no secondary phases were identified which suggests that the NPs were of high purity. The average crystallite size of both pure and Mn-doped CaWO$_4$ NPs were calculated using Scherrer's formula and by considering all the peaks. The average sizes were found to be 34 ± 0.6 nm in case of pure and that of Mn-doped CaWO$_4$ NPs were almost the same. In case of undoped CaWO$_4$ NPs the lattice parameter was found to be $a = 5.367$ Å and $c = 11.442$ Å, and for all Mn (1%–4%)-doped CaWO$_4$ NPs are also in the same range $a = 5.324$ Å and $c = 11.412$ Å. In our earlier work on rare earth doped

Figure 2. (a) Optical absorption spectra of (a) $CaWO_4$, (b) 1% Mn: $CaWO_4$, (c) 2% Mn: $CaWO_4$, (d) 3% Mn: $CaWO_4$ and (e) 4% Mn: $CaWO_4$ NPs respectively in the wavelength range of 200–400 nm and (b) larger wavelengths 450–600 nm.

$CaWO_4$ NPs the lattice parameters values were found to be in the similar range [23]. Morphological studies and elemental composition of Mn-doped $CaWO_4$ NPs were carried out on these NPs using field emission scanning electron microscope, EDAX and ICP-AES measurements (see supplementary information is available online at stacks.iop.org/PS/95/035806/mmedia). The sizes obtained were in good agreement with that of XRD measurements.

Figure 2(a) shows the optical absorption spectra of pure and Mn doped $CaWO_4$ NPs. Two peaks appeared at around 240 and 350 nm which were attributed to band-edge of $CaWO_4$ and WO_3^- [24]. Similar peaks were obtained in case of pure $CaWO_4$ NPs and also compared with that of its bulk counterpart [25]. However, compared to the bulk material, there is a blue shift in the band-edge position which is attributed to confinement effects. However, upon Mn incorporation into the lattice of $CaWO_4$ NPs a red shift in the peak is observed when compared with undoped NPs. The redshift is attributed enhanced reactivity of the precursor used in the synthesis process [22]. The band gap were estimated by using Kubelka–Munk function for undoped and Mn doped NPs, which were found to be in the range of 3.60 eV (340 nm) to 3.53 eV (351 nm) (see supporting information). Here also a redshift in terms of wavelength has been observed due to Mn incorporation. Moreover, upon addition of Mn a new peak around 530 nm was evident (figure 2(b)) [26]. The appearance of this peak is attributed to Mn related *d–d* transitions. In case of bulk material these transitions (*d–d*) are actually forbidden, however in nano regime due to quantum confinement effect these peaks are observed quite often [26–30].

To throw a further light on the incorporation of Mn in the host lattice ESR was carried out. ESR is more preferred method to study the presence of impurity inside the material [31]. This method not only helps to conclude the spin and charge state of an impurity but also its symmetry, environment around the structure, and its interaction with the crystal lattice. As shown in figure 3 for lower concentrations of Mn in $CaWO_4$ NPs a six line hyper fine splitting was revealed in ESR spectra. This hyper fine spectrum is the characteristics of
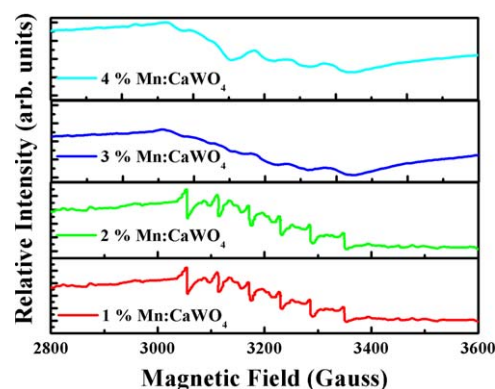
Figure 3. EPR spectra of Mn-$CaWO_4$ NPs with 3% and 4% of Mn respectively.

Mn in +2 state similar kind of spectrum were also reported by doping Mn in different materials [29, 30, 32]. For higher concentrations (as shown in figure 3) the sharpness of the peaks decreased but still six line splitting was observed. Upon calculation of Lande's *g* factor and hyper fine splitting constant it is observed that the values are $g = 2.0042$ and $g = 2.0093$ and that of hyperfine splitting constant $|A|$ changed from 67.1×10^{-4} to 73.2×10^{-4} cm. The high value of hyperfine splitting constant is attributed to Mn^{2+} ions which are bounded to the surface of the NPs. This also indicates less symmetry of the system and poses a serious limit on the doping level and could be the reason of the accumulation of Mn ions at the grain surfaces, as deduced from the ESR measurements. In other words, in heavily doped $CaWO_4$ NPs there could be an appearance of accumulation of Mn ions at the surface. This enhanced hyperfine splitting leads to decrease in covalence, as well as decrease in coupling between the ground state of Mn and *sp*-states of the NPs. Thus less covalence can be anticipated for Mn positioned at or near the surface.

Photoluminescence (PL) emission and excitation (PLE) spectra were recorded for pure and Mn doped $CaWO_4$ NPs. To record the PL emission spectra, all the samples were excited with 350 nm figure 4. In case of pure $CaWO_4$ NPs
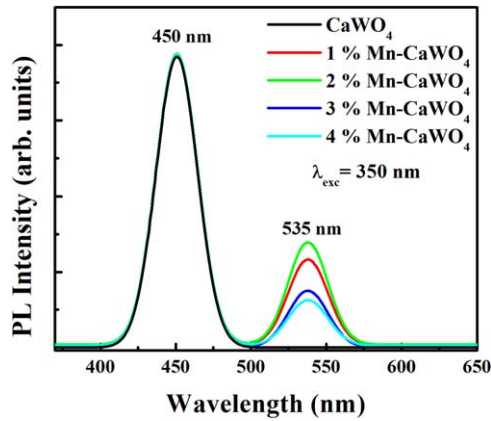
Figure 4. PL spectra of (a) $CaWO_4$, (b) 1% Mn: $CaWO_4$, (c) 2% Mn: $CaWO_4$, (d) 3% Mn: $CaWO_4$ and (e) 4% Mn: $CaWO_4$ NPs with excitation wavelength of 350 nm.

only one peak was observed at around 450 nm and is attributed to $CaWO_4$ emission [33]. However, in case of Mn doped $CaWO_4$ NPs the emission spectra have two peaks centred at 450 and 535 nm. The peak corresponding to 535 nm is attributed to *d–d* transition of Mn^{2+} ions. It can be seen from the figure that with increase in concentration of Mn the intensity of the peak went on increasing initially and dropped down at higher concentration. The decrease in peak intensity can be attributed to accumulation of more number of Mn ions on the surface of the $CaWO_4$ NPs [30].

PLE spectra of both band edge and Mn related emission is as shown in figure 6. In case of band-edge related excitation spectra which are recorded at 450 nm. Two peaks corresponding to band-edge as well as WO_3- related was observed. In almost all the cases whether undoped or Mn doped $CaWO_4$ NPs similar PLE spectra was recorded at 450 nm (figure 5(a)). In case of Mn related excitation (535 nm) spectra four peaks at 319, 371, 449 and 477 nm were observed. These peaks were attributed to $^6A_1(S) \rightarrow ^4A_1$, $^4E(4\,G)$, $^6A_1(S) \rightarrow ^4T_2(4\,G)$, and $^6A_1(S) \rightarrow ^4T_1(4\,G)$ which are *d–d* transition of Mn (figure 5(b)). However there is shift in the peak positions

when compared with Mn in other materials and can be attributed to delocalization of Mn^{2+} ions in the lattice host lattcie [34–36].

Time dependent photoluminescence measurements were carried out on these NPs. Figure 6 reveals decay profiles of the NPs one recorded at band edge (450 nm) and the other at Mn site (535 nm). The life time values at band edge site were in the range of micro seconds (around 17 μs) [37]. Upon doping Mn in $CaWO_4$ NPs no decrease in life time was observed which indicates that due to addition of Mn there is no quenching in band-edge emission. PL spectra (figure 4) also revealed the same. While probing at 535 nm, (at Mn site) the recombination lifetime value was found to be in milliseconds (4.3 ms). This larger life time values of Mn confirms that the Mn ion is present in the host lattice and the spin forbidden *d–d* transitions show a slower recombination time [22, 38, 39].

4. Conclusions

An attempt has been made to synthesis and study optical properties of Mn:$CaWO_4$ NPs by using hydrothermal method. The concentrations of Mn in $CaWO_4$ NPs were varied from 1% to 4% by weight with respect to Ca. Optical absorption peak revealed both band edge as well as Mn related (*d–d*) transition. Incorporation of Mn at substitutional site and indicating that Mn is in 2+ state was revealed by ESR measurements. Room temperature photoluminescence emission (PL) and excitation (PLE) spectroscopies were carried out to understand the interactions of *sp-d* levels. PL spectra revealed the presence of both band-edge ($\sim$450 nm) and Mn^{2+} related orange luminescence ($\sim$535 nm). Time dependent photoluminescence (TDPL) studies were also carried out and the life time values obtained were in the range of 435 μs which was similar to when compared with Mn in other systems. Thus TDPL further strengths the presence of Mn in $CaWO_4$ NPs.

(a)

(b)
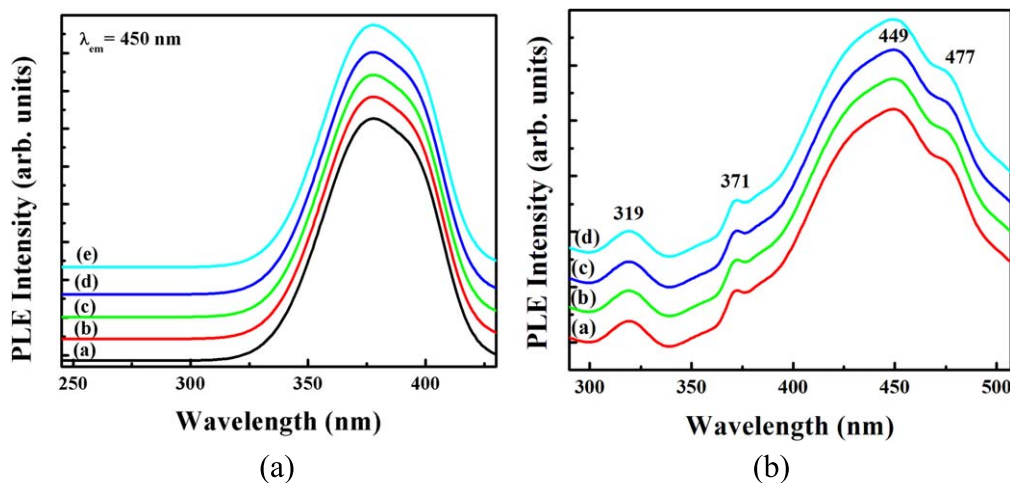
Figure 5. (a) PLE spectra of (a) $CaWO_4$, (b) 1% Mn: $CaWO_4$, (c) 2% Mn: $CaWO_4$, (d) 3% Mn: $CaWO_4$ and (e) 4% Mn: $CaWO_4$ NPs with emission wavelength of 450 nm. (b) PLE spectra of (a) 1% Mn: $CaWO_4$, (b) 2% Mn: $CaWO_4$, (c) 3% Mn: $CaWO_4$ and (d) 4% Mn: $CaWO_4$ NPs with emission wavelength of 535 nm.
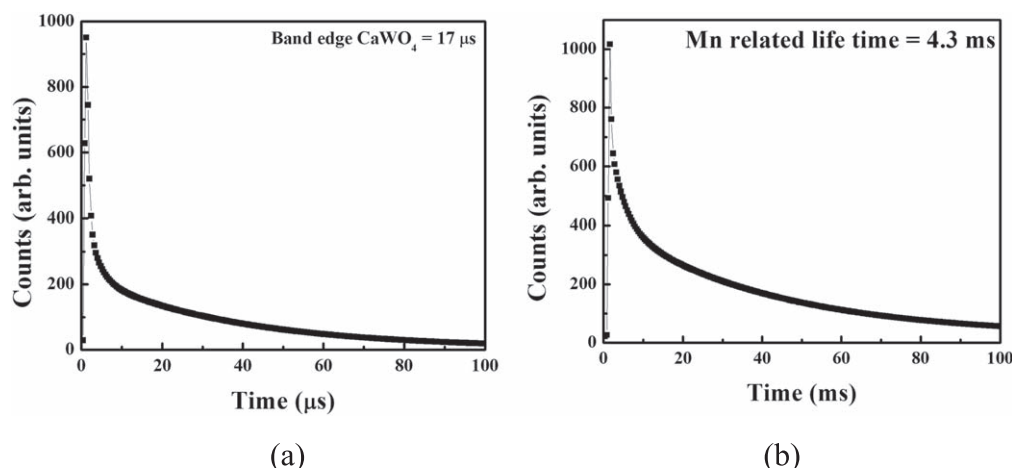
Figure 6. Time dependent photoluminescence of $CaWO_4$ and $Mn:CaWO_4$ NPs (a) band edge and (b) Mn related site.

Acknowledgments

ORCID iDs

Ch Rajesh https://orcid.org/0000-0002-7022-0549

References

[1] Zawawi S M M, Yahya R, Hassan A, Mahmud H N M E and Daud M N 2013 Structural and optical characterization of metal tungstates (MWO_4; M = Ni, Ba, Bi) synthesized by a sucrose-templated method *Chem. Cent. J.* **7** 80

[2] Purnendu P, Karthik T N and Manivannan V 2008 Synthesis and characterization of metal tungstates by novel solid-state metathetic approach *J. Alloys Compd.* **465** 380

[3] Forgaciu F, Popovici E J, Ungur L and Vadan M 2000 Calcium tungstate phosphors with well-defined particle sizes *Proc. SPIE Int. Soc. Opt. Eng.* **124** 4068

[4] Nazarov M V, Jeon D Y, Kang J H, Zamoryanskara M V and Tsukerblat B S 2004 Luminescence properties of europium–terbium double activated calcium tungstate phosphor *Solid State Commun.* **131** 307

[5] Cebrian S, Coron N, Dambier G, Marcillac P, Garcia E and Villar J A 2003 First underground light versus heat discrimination for dark matter search *Phys. Lett.* B **563** 48

[6] Zhai R, Wang H, Yan H and Yoshimura M 2006 Preparation of crystalline $CaWO_4$ thin films by chemical bath deposition *J. Cryst. Growth* **289** 647

[7] Sun L, Cao M, Wang Y, Sun G and Hu C 2006 The synthesis and photoluminescent properties of calcium tungstate nanocrystals *J. Cryst. Growth* **289** 231

[8] Lou Z and Cocivera M 2002 Cathodoluminescence of $CaWO_4$ and $SrWO_4$ thin films prepared by spray pyrolysis *Mater. Res. Bull.* **37** 1573

[9] Phuruangrata A, Thongtema T and Thongtema S 2010 Synthesis, characterization and photoluminescence of nanocrystalline calcium tungstate *J. Exp. Nanosci.* **5** 263

[10] Shan Z, Wang Y, Ding H and Huang F 2009 Structure-dependent photocatalytic activities of MWO_4 (M = Ca, Sr, Ba) *J. Mol. Catal.* A **302** 54

[11] Cavalcante L S, Sczancoski J C, Lima L F, Espinosa J J W M, Pizani P S, Varela J A and Longo E 2009 Synthesis, characterization, anisotropic growth and photoluminescence of $BaWO_4$ *Cryst. Growth Des.* **9** 1002

[12] Kaowphong S, Thongtem T and Thongtem S 2010 Effect of solvents on the microstructure of $CaWO_4$ prepared by a solvothermal synthesis *J. Ceram. Process. Res.* **11** 432

[13] Pechini M P 1967 *US Patent* 3330697

[14] Kwan S, Kim F, Akana J and Yang P 2001 Synthesis and assembly of $BaWO_4$ nanorods *Chem. Commun.* **5** 447

[15] Singh B P and Singh R A 2015 Color tuning in thermally stable Sm^{3+} activated $CaWO_4$ nanophosphors *New J. Chem.* **39** 4494

[16] Xia Q, Zho Q and Li M 2010 Synthesis and photoluminescence properties of Sm^{3+} doped $CaWO_4$ nanoparticles *J. Lumin.* **130** 1092

[17] Alencar L D S, Lima N A, Alexandre M, Probst L F D, Batalha D C, Rosamaninho M G, Fajardo H V, Balzer R and Bernard M I B 2018 Effect of different synthesis methods on textural properties of $CaWO_4$ and its catalytic properties in the toluene oxidation *Mater. Res.* **21** 2072

[18] Suneeta P, Ramana M V and Rajesh C 2017 Synthesis and characterization of Sm and Pr-doped $CaWO_4$ nano-crystals *Mater. Res. Express* **4** 045013

[19] Suneeta P, Ramana M V and Rajesh C 2017 Nd-doped CaWO4 nanocrystals—synthesis and characterization *Mater. Res. Express* **4** 085020

[20] Karolewicz M, Fuks H and Tomaszewicz E 2019 Synthesis and thermal, optical and magnetic properties of new Mn^{2+} doped and Eu^{3+} co-doped scheelites *J. Therm. Anal. Calorim.* **1** 13

[21] Rajesh C, Phadnis C V, Sonawane K G and Mahamuni S 2015 Generation of white light from codoped (Cu and Mn) ZnSe QDs *J. Exp. Nanosci.* **10** 1082

[22] Suneeta P, Ramana M V and Rajesh C 2018 Synthesis and characterization of rare-earth–doped calcium tungstate nanocrystals *Euro Phys. J. Plus* **133** 59

[23] Treasaway M J and Powell R C 1974 Luminescence of calcium tungstate crystals *J. Chem. Phys.* **61** 4003

[24] Mai M and Feldmann C 2012 Microemulsion-based synthesis and luminescence of nanoparticulate $CaWO_4$, $ZnWO_4$, $CaWO_4:Tb$, and $CaWO_4:Eu$ *J. Mater. Sci.* **47** 1427

[25] Furdyna J K 1988 Diluted magnetic semiconductors *J. Appl. Phys.* **64** R29

[26] Norris D J, Yao N, Charnock F T and Kennedy T A 2001 High quality manganese doped ZnSe nanocrystals *Nano Lett.* **1** 3

[27] Suyver J F, Wuister S F, Kelly J J and Meijerink A 2000 Luminescence of nanocrystalline ZnSe:Mn^{2+} *Phys. Chem. Chem. Phys.* **2** 5445

[28] Norman T J, Magana D, Wilson T, Burns C and Zhang J Z 2003 Optical and surface structural properties of Mn^{2+} doped ZnSe nanoparticles *J. Phys. Chem.* B **107** 6309

[29] Zu L, Norris D J, Kennedy T A, Erwin S C and Efros A L 2006 Impact of ripening on manganese doped ZnSe nanocrystals *Nano Lett.* **6** 334

[30] Bravo D and Lopez F J 1999 The EPR technique as a tool for understanding of laser systems: the case of Cr^{3+} and Cr^{4+} ions in $Bi_4Ge_3O_{12}$ *Opt. Mater.* **13** 141

[31] Lad A D, Rajesh C, Khan M, Ali N, Gopalakrishnan I K, Kulshrestha S K and Mahamuni S 2007 Magnetic behavior of manganese-doped ZnSe quantum dots *J. Appl. Phys.* **101** 103906

[32] Suna L, Cao M, Wang Y, Suna G and Hua C 2006 The synthesis and photoluminescence properties of calcium tungstate nanocrystals *J. Cryst. Growth* **289** 231

[33] Mahamuni S, Lad A D and Patole S 2008 Photoluminescence properties of manganese-doped zinc selenide quantum dots *J. Phys. Chem.* C **112** 2271

[34] Chen W, Sammynaiken R, Huang Y, Malm J O, Wallenberg R, Bovin J O, Zwiller V and Kotov N A 2001 Crystal field, phonon coupling and emission shift of Mn^{2+} in ZnS:Mn nanoparticles *J. Appl. Phys.* **80** 1120

[35] Kumar R A, Prasad M V V K S, Kumar G K, Venkateswarlu M and Rajesh C 2019 Tuning of emission from copper-doped ZnSe quantum dots *Phys. Scr.* **94** 115806

[36] Rajesh C, Lad A D, Ghangrekar A and Mahamuni S 2008 Exciton recombination dynamics in zinc selenide quantum dots *Solid State Commun.* **148** 435

[37] Kennedy T A, Glaser E R, Klein P B and Bhargava R N 1995 Symmetry and electronic structure of the Mn impurity in ZnS nanocrystals *Phys. Rev.* B **52** R14356

[38] Rajesh C, Phadnis C V, Sonawane K G and Mahamuni S 2015 Synthesis and optical properties of copper-doped ZnSe quantum dots *Phys. Scr.* **90** 015803

[39] Feldmann C, Justel T, Ronda C R and Schmidt P J 2003 Inorganic luminescent materials: 100 years of research and application *Adv. Funct. Mater.* **13** 511